SNOW ACCUMULATION AND ABLATION IN DIFFERENT CANOPY STRUCTURES AT A PLOT SCALE: USING DEGREE-DAY APPROACH AND MEASURED SHORTWAVE RADIATION

MICHAL JENÍČEK, ONDŘEJ HOTOVÝ, ONDŘEJ MATĚJKA

Charles University, Faculty of Science, Department of Physical Geography and Geoecology, Czech Republic

ABSTRACT

The knowledge of water volume stored in the snowpack and its spatial distribution is important to predict the snowmelt runoff. The objective of this study was to quantify the role of different forest types on the snowpack distribution at a plot scale during snow accumulation and snow ablation periods. Special interest was put in the role of the forest affected by the bark beetle (*Ips typographus*). We performed repeated detailed manual field survey at selected mountain plots with different canopy structure located at the same elevation and without influence of topography and wind on the snow distribution. A snow accumulation and ablation model was set up to simulate the snow water equivalent (SWE) in plots with different vegetation cover. The model was based on degree-day approach and accounts for snow interception in different forest types.

The measured SWE in the plot with healthy forest was on average by 41% lower than in open area during snow accumulation period. The disturbed forest caused the SWE reduction by 22% compared to open area indicating increasing snow storage after forest defoliation. The snow ablation in healthy forest was by 32% slower compared to open area. On the contrary, the snow ablation in disturbed forest (due to the bark beetle) was on average only by 7% slower than in open area. The relative decrease in incoming solar radiation in the forest compared to open area was much bigger compared to the relative decrease in snowmelt rates. This indicated that the decrease in snowmelt rates cannot be explained only by the decrease in incoming solar radiation. The model simulated best in open area and slightly worse in healthy forest. The model showed faster snowmelt after forest defoliation which also resulted in earlier snow melt-out in the disturbed forest.

Keywords: snow accumulation, snowmelt, degree-day model, forest disturbance

Received 15 September 2016; Accepted 11 November 2016; Published online 27 February 2017

1. Introduction

The effects of forest cover on snow accumulation and ablation have been widely studied in last decades. However, at a catchment scale, there is still no comprehensive explanation how sensitive is snowmelt runoff to changes in mountain forest cover (Pomeroy et al. 2012). At a small spatial scale, the snow accumulation and ablation is controlled dominantly by local topography and vegetation (Jost et al. 2007). The differences between snow water equivalent (SWE) in a forest compared to open area have been described in many studies. These differences may be explained by 1) the increase in snow interception on forest canopy which reduces snow accumulation on the earth surface due to snow sublimation and evaporation (Essery et al. 2003; Varhola et al. 2010), and 2) the decrease in incoming solar radiation with increasing canopy density (Ellis and Pomeroy 2007; Hribik et al. 2012). Generally, forest significantly affects energy exchange between the snowpack and atmosphere. The forest reduces the ablation rates by attenuating solar radiation and near-surface wind speed (López-Moreno and Stähli 2008; Molotch et al. 2009).

Many studies showed that snow accumulated in forests is by 40–50% lower than that in nearby open areas (see e.g. Bartík et al. 2014; Jenicek et al. 2016, 2015; Jost et al. 2007; Stähli and Gustafsson 2006). The study performed in experimental forested mountain plots in central Europe showed that up to 60% of cumulative snowfall was intercepted and sublimated (Holko et al. 2009).

The shortwave radiation is reflected on tree needles causing its reduction under forest canopy. Up to 90% of the incoming shortwave radiation is reflected back to the atmosphere in case of dense coniferous forest (e.g. Aubin et al. 2011; Sicart et al. 2004). This reducing effect is important during snow ablation period causing faster snowmelt in open area compared to forest.

Previously mentioned effects are widely influenced by changes in canopy structure caused by harvesting or various forest disturbances such as windstorms and the bark beetle attacks. The changes in forest structure significantly affect the snow interception and amount of shortwave and longwave radiation. It strongly affects both the snow accumulation (with expected increase in maximum SWE due to reduced snow interception) and snow ablation (with expected faster snowmelt after forest decay due to increasing shortwave radiation), although the impacts are not fully described and may be influenced by several other parameters (Biederman et al. 2014; Pomeroy et al. 2012).

The objective of our study was to quantify the role of different forest types on the snowpack distribution at a

https://doi.org/10.14712/23361980.2017.5
Jeníček, M. – Hotový, O. – Matějka, O. (2017):
Snow accumulation and ablation in different canopy structures at a plot scale: using degree-day approach and measured shortwave radiation
AUC Geographica, 52, No. 1, pp. 61–72

plot scale during snow accumulation and snow ablation periods. More specifically, we performed detailed manual filed survey at selected plots located at the same elevation and without influence of topography and wind on the snow distribution. Thanks to this sampling configuration it was possible to explore the effect of canopy structure on the snowpack distribution separately. This is not a new topic, but our study focused more on the effect of different forest types including disturbed forest due to the bark beetle during both snow accumulation and snow ablation periods. We benefit from detailed repeated manual snow depth and SWE measurement supported by continuous monitoring of meteorological variables including snow depth, SWE and shortwave radiation (both incoming and reflected).

2. Material and methods

2.1 Study area and data monitoring

We performed detailed field survey of snow depth, snow density and SWE in four plots located in the Ptačí Brook catchment, which is an experimental catchment of the Charles University (Fig. 1). The Ptačí Brook catchment covers an area of 4 km^2 and it is located in the Šumava Mountains (Bavarian forest) in the southwest part of the Czech Republic. The catchment is located from 1130 to 1330 m a.s.l with prevailing west, north and east oriented slopes with mean slope gradient 6° (with maximum up to 30°). The Ptačí Brook has snow-dominating runoff regime with highest runoff volume approximately from late March to beginning of May caused by melting snow. The dominant tree species is Norway spruce (*Picea abies*), although large parts of forests were damaged by the bark beetle (*Ips typographus*). Both windstorms and the bark beetle are the main factors causing land cover changes in the Šumava Mountains, which has an effect on interception, evaporation and consequently runoff (Kliment et al. 2011; Kocum et al. 2016; Langhammer et al. 2015a, 2015b).

Studied catchment is equipped with measurement of precipitation (only warm period), air, snow and soil temperature, air moisture, shortwave and longwave radiation, SWE and ultrasonic measurement of snow depth. The winter precipitation using heated rain gauge is measured at the meteorological station Modrava which is located 4 km from the Ptačí Brook catchment. The SWE is measured directly in the study catchment in open area using Snow Pack Analyzer SPA (Sommer Messtechnik). This device uses three strips measuring the impedance of the snowpack and calculates the ratio of ice, air and liquid water in the snowpack which is further used to calculate the snow density. Two strips are placed horizontally in 5 cm and 25 cm above the earth surface and the third strip is placed diagonally providing the aggregate information from the entire snow column.

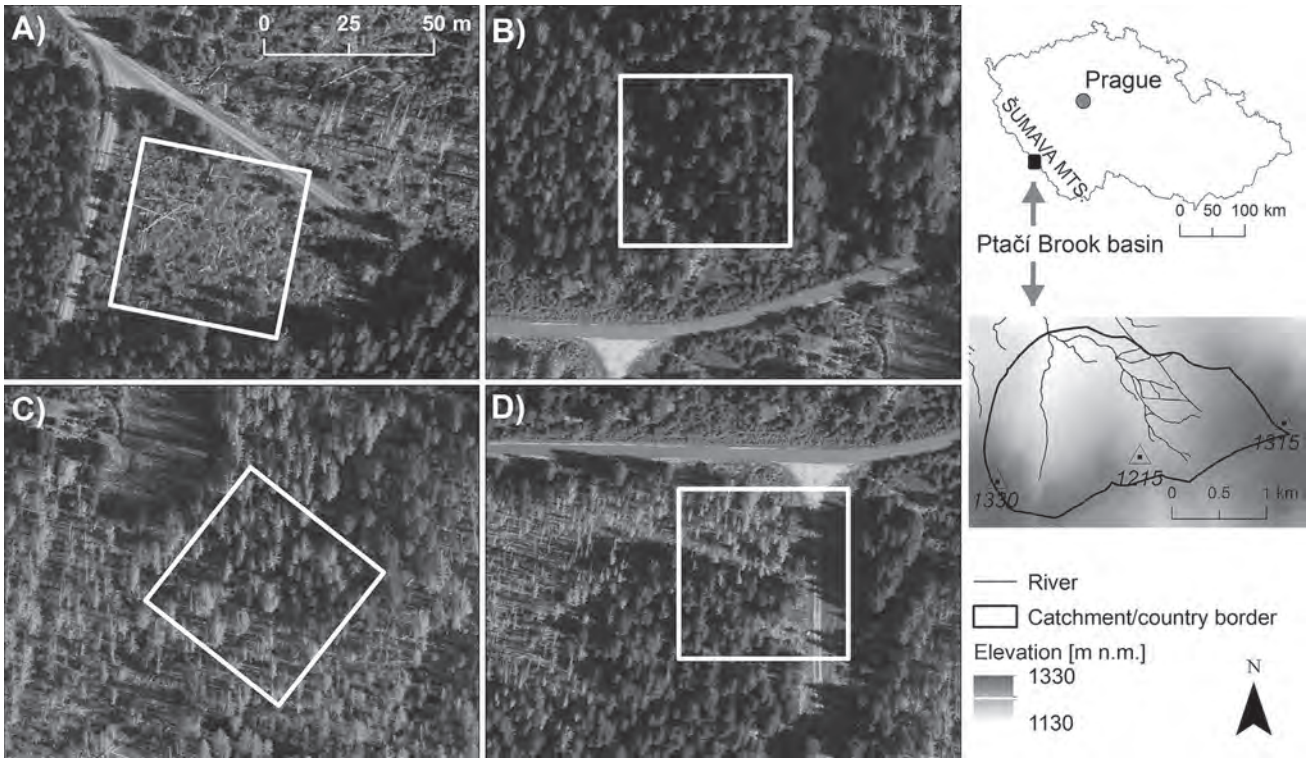

Fig. 1 Geographical location of the Ptačí Brook catchment. Airborne images of individual sampling sites show their vegetation structure; open area (A), healthy coniferous forest (B), disturbed forest due to the bark beetle (C) and mixed vegetation (D) (Data: Czech Office for Surveying, Mapping and Cadastre ČÚZK).

The incoming and reflected shortwave and longwave radiation is measured using CNR4 Net Radiometer (Kipp and Zonen). This device consists of two pyranometers (first is oriented upward, second is oriented downward) and two pyrgeometers (same configuration as for pyranometers). Thanks to this configuration, the global and reflected radiation is measured enabling albedo calculation. The device was supplemented with air temperature measurement. We used three net radiometers placed in open area (neighboring area to plot A, Fig. 1), healthy coniferous forest (plot B) and disturbed coniferous forest due to the bark beetle (plot C).

2.2 Sampling strategy and spatial data interpolation

We applied a simple sampling design at a plot scale at four locations representing major vegetation categories typical for the study area; open area (plot A), healthy (green) coniferous forest (plot B) and disturbed forest due to the bark beetle (plot C). First three plots represent these three categories; the fourth plot has a mixed vegetation consisting with all previously specified vegetation categories (plot D, Fig. 1).

Each plot has an area 50 × 50 meters. The snow depth was manually measured each tenth meter which results in raster containing 36 values of the snow depth. The bulk snow density was measured five times using a snow tube and a digital scale (measurement resolution 10 g). The five points with snow density measurement were located uniformly within the plot; one in the middle and the four were located near every corner always 10 meters from the plot edges (inside the plot). The mean bulk snow density was used to calculate the SWE in each raster cell resulting in 36 SWE values for each plot.

Manual field surveys of snow depth, snow density and SWE were carried out five times during one winter season 2015/2016; 4 February 2016, 19 February 2016, 19 March 2016, 1 April 2016 and 6 April 2016. The first three sampling dates represent snow accumulation period (interrupted with partial snowmelt due to rain-on-snow event) with maximum snow storage close to 19 March 2016. A period between last two sampling dates (01 Apr – 06 Apr) represents snowmelt caused by high air temperature and high solar radiation without precipitation. This period represents the major snowmelt period in the study area.

Data were interpolated using Natural neighbor method. Interpolated rasters containing SWE data from all plots in 1 Apr 2016 and 6 Apr 2016 were used to calculate ablation rates by subtracting the rasters from each other. The size of raster pixel was set to 0.5 m.

2.3 The snow accumulation and ablation model based on the degree-day approach

A snow accumulation and ablation model was set up to simulate the snow evolution in plots with different vegetation cover. Although, we are aware that the snow ablation is driven by the complex energy balance, our aim was to apply simple procedures to enable easier application in areas without detail meteorological monitoring. The simplified equation of the model calculating the snow water equivalent S for time interval t is (Eq. 1):

$$S_t = S_{t-1} + P_t - A_r - m_f\,(T_t - T_{cmelt}), \quad (1)$$

All parameters with detailed explanation are listed in Table 1. The model was written in R programming language (R Core Team 2016). The model accounts for snow and rain interception using multiplication factors applying for precipitation P (ICFS, Interception Correction Factor for Snow; ICFR, Interception Correction Factor for Rain). Different factors for different vegetation cover were applied. In case of our model, the initial value of the ICFS was based on measured differences between SWE in the open area (plot A) and in other sampling locations. Solid precipitation was adjusted for undercatch using Snowfall Correction Factor (SFCF) due to wind affecting the capture of the snow flake into a rain gauge. Because the data of precipitation phase were not available, the differentiation between snow and rain has been done by a threshold temperature (T_{crain}) which was set up to 1 °C representing widely used value. Constant ablation rate A_r

Tab. 1 Parameters of the snow accumulation and snow ablation model.

T [°C]	Air temperature (usually daily mean). The data from meteorological station in Ptačí Brook were used.
P [mm]	Precipitation (usually daily sum). The data from heated rain gauge placed in meteorological station Modrava (4 km from Ptačí Brook) were used
SFCF [–]	Snowfall Correction Factor enables to account for snow undercatch
T_{cmelt} [°C]	Critical temperature for snowmelt initiation (degree-day approach)
T_{crain} [°C]	Critical temperature differentiating between snow and rain
LR [°C/100 m]	Lapse rate accounting for temperature decrease with elevation (typically 0.6 °C per 100 m)
ICFS [–]	Interception Correction Factor for Snow accounting for snow interception in vegetation with different canopy structure
ICFR [–]	Interception Correction Factor for Rain accounting for rain interception in vegetation with different canopy structure
A_r [mm]	Constant ablation rate used to account for snow ablation caused by sublimation and ground melt. Constant ablation rate is applied only for snow accumulation (for snowmelt, all processes causing ablation are considered within the melt factor m_f)
m_f [mm °C^{-1} d^{-1}]	Melt factor or degree-day factor representing the SWE decrease in a day caused by the air temperature T change by 1 °C compared to the critical air temperature T_{cmelt} in which the melting process begins

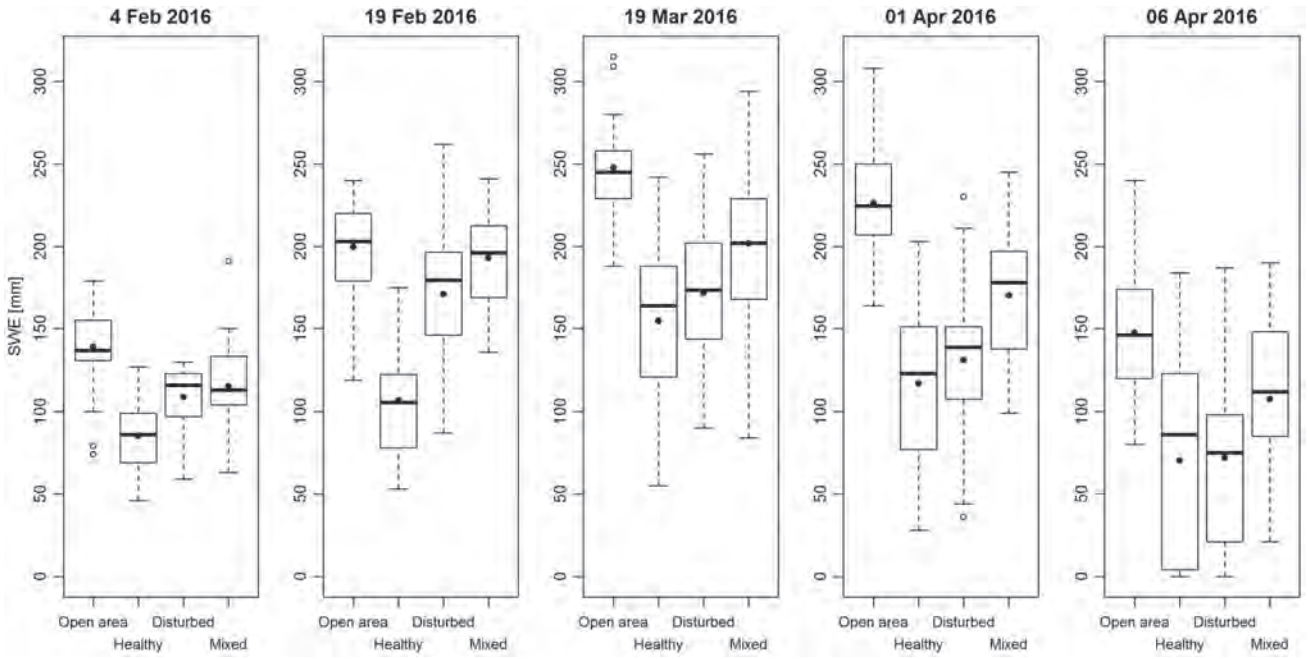

Fig. 2 The SWE in study plots in relation to vegetation. Boxes represent 25% and 75% percentile (with median as a thick line), whiskers represent 1.5 multiplier of interquartile range (IQR), black points represent mean value and transparent points represent outliers (higher than 1.5 of IQR, if existing).

was applied for snow accumulation periods to account for ground melt and sublimation. Constant ablation was not applied for snowmelt period since it is included in melt factor m_f.

The degree-day approach (see e.g. Hock 2003; Jenicek et al. 2012) was used in this study to simulate the snowmelt in plots with different vegetation cover. The degree-day approach represents the simplified energy balance of the snowpack, which is described using the air temperature T and melt factor m_f.

The melt factors for different types of vegetation were calculated based on measured SWE decreases between last two sampling dates where there was no influence of precipitation. Air temperature measured at meteorological station located in the immediate vicinity of sampling locations was used in the model. Critical temperature T_{cmelt} was set up to 0 °C in this case.

The parameters related to interception and critical temperatures were calibrated based on measured SWE in all sampling locations in order to get the best simulation fitted to observed data. The data from snowpack analyzer SPA and snow depth sensor were used to estimate the SFCF. The melt factors were not calibrated since they were calculated based on measured data. The validation of the model was not possible since data from one winter season were available at the time of study processing. The Nash-Sutcliffe efficiency NSE was used to assess the goodness-of-fit of the model (Nash and Sutcliffe 1970). A value 1 indicates perfect fit of simulations with observations, value 0 means that the model is as good as the mean of observed data.

3. Results

3.1 The development of SWE and snow density at individual plots in time

The development of SWE at individual plots in winter season 2015/2016 is displayed in Fig. 2. Until 19 March 2016 there was an increase in snow storage in all plots and this date was close to the date with maximum snow accumulation (although the snow accumulation period was influenced by several partial thawing periods). The average SWE measured in the date with maximum snow storage was 322 mm in open area, 242 mm in healthy forest, 256 mm in forest disturbed by the bark beetle and 294 mm in plot with mixed vegetation (healthy and disturbed coniferous forest and open area).

The SWE in the healthy forest was on average by 41% lower than in open area during accumulation period (first three sampling dates). The disturbed forest caused the SWE reduction by 22%, which clearly indicated reducing snow interception after forest defoliation and thus increasing snow storage. It is expected that the snow interception effect is likely to decrease in disturbed forest due to the gradual fall of branches and trunks, and thus snow accumulation increases.

The snow ablation in the healthy forest was slower than in open area and in disturbed forest. The SWE in open area decreased by 79 mm from 1 Apr 2016 to 6 Apr 2016 while the SWE decreased only by 47 mm in healthy forest and by 60 mm in disturbed forest in the same period. The dominant process which explains mentioned differences

is reduced amount of incoming shortwave radiation in forest sites. We can expect faster snowmelt in disturbed forest next years due to further decay of the forest and thus increasing amount of incoming solar radiation.

Similarly to SWE, the snow density also differs in different types of vegetation. As expected, there was lower snow density in all vegetation categories during snow accumulation compared to snow ablation (Fig. 3). The median of snow density was lowest in the healthy forest, although the variability was highest when compare all vegetation categories. In forest disturbed by the bark beetle, the snow density slightly increased compared to the healthy forest while the variability decreased. The highest snow density was expectedly in open areas and in the plot with mixed vegetation cover, probably due to the combined effect of wind and higher incoming solar radiation. Generally, the snow density variability is caused by combined effects of 1) snow interception and canopy drip, 2) snow redistribution by wind, 3) equi-temperature metamorphism and 4) melt-freeze cycle metamorphisms. Mentioned effects additionally cause the increasing snow density at specific localities in time (with increasing day of year).

3.2 The SWE variability at a plot scale

To describe the variability of SWE at a plot scale we used the coefficient of variation C_v (Fig. 4). The C_v was calculated using standard deviation of SWE values (36 values) at specific sampling plot divided by its mean. The higher was the value, the higher was the SWE variability at the specific sampling plot. The C_v was calculated for each plot and for each sampling date.

The results showed general higher variability during snowmelt than during snow accumulation period. This was expected since the snowpack is influenced by even more factors during snow ablation than during snow accumulation (such as increase in solar radiation). The results also showed higher variability in the forest than in other vegetation categories which indicated the influence of canopy structure on the snowpack variability.

The histogram of SWE values for different canopy covers and dates is shown in Fig. 5. The individual lines represent the SWE distribution in individual sampling dates and in different vegetation. Histograms of SWE at the time of each sampling date showed that the distribution and the variability changed in the course of the accumulation and ablation season. It is clear that variability markedly increased during snowmelt season (last two sampling dates) which is indicated by histograms with wider base. Both Fig. 4 and Fig. 5 show the fact, that the SWE variability was generally higher in forest sites than in open area.

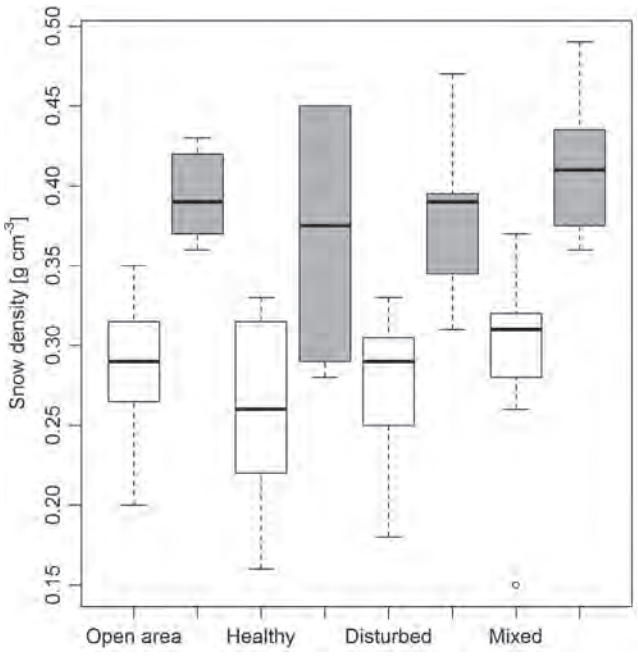

Fig. 3 The snow density in individual plots. White box plots represent sampling dates during snow accumulation; grey box plots represent snowmelt dates. Boxes represent 25% and 75% percentile (with median as a thick line), whiskers represent 1.5 multiplier of IQR.

3.3 Ablation rates in relation to forest type and shortwave radiation

The snowmelt rates and melt factors m_f were calculated using data measured in 1 April and 6 April. These sampling dates define the period with high air temperature and high amount of incoming solar radiation. The snowmelt in the plot with disturbed forest markedly increased and its snowmelt rates was almost same as in open area (16.1 mm d^{-1} for open area; 15 mm d^{-1} for disturbed forest, table 2). The average snowmelt rate in healthy forest with dense treetops was much lower (10.9 mm d^{-1}). The spatial differences in snowmelt rates in forested plots were probably caused by different amount of shortwave radiation resulting from different canopy structure and thus shading effects (Fig. 6). Additionally, the snowmelt in the open area was influenced by surrounding trees, especially on its edges. These surrounding trees affected non-uniform snow ablation with higher snowmelt rates especially in the north part of the plot due to the reducing shading effect. Additionally, the presence of surrounding trees probably caused wind speed reduction and thus the snow redistribution due to wind was minimized.

The ablation rates and melt factor m_f as a key parameter in degree-day approach showed different snowmelt dynamics in different forest types (Table 2, Fig. 6, Fig. 7). The melt factors increased due to the increase in incoming solar radiation (caused by sparser canopy cover) and thus decrease of shading effects. The snow ablation in healthy forest was by 32% slower compared to sites in open area. On the contrary, the snow ablation in disturbed forest (due to the bark beetle) was on average only by 7% slower than in open area which indicates considerable increase in incoming solar radiation after forest defoliation. It is

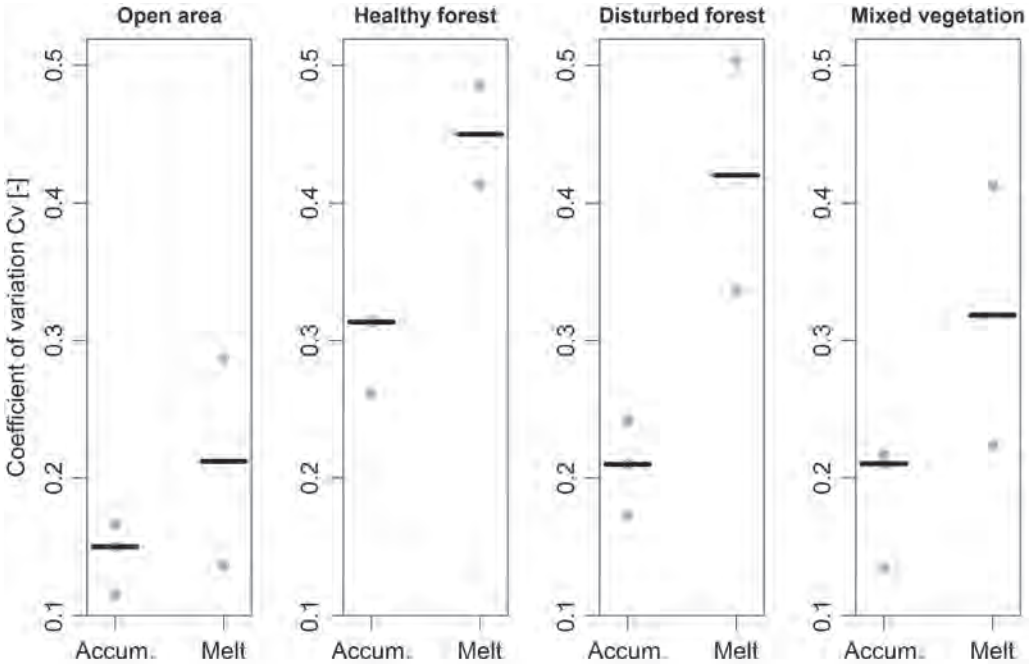

Fig. 4 The coefficients of variation C_v describing the SWE variability at a site level in an open area, healthy forest, disturbed forest and mixed vegetation in the Ptačí Brook catchment during snow accumulation and snow ablation period. The grey points indicate the individual C_v, horizontal lines indicate the median of C_v.

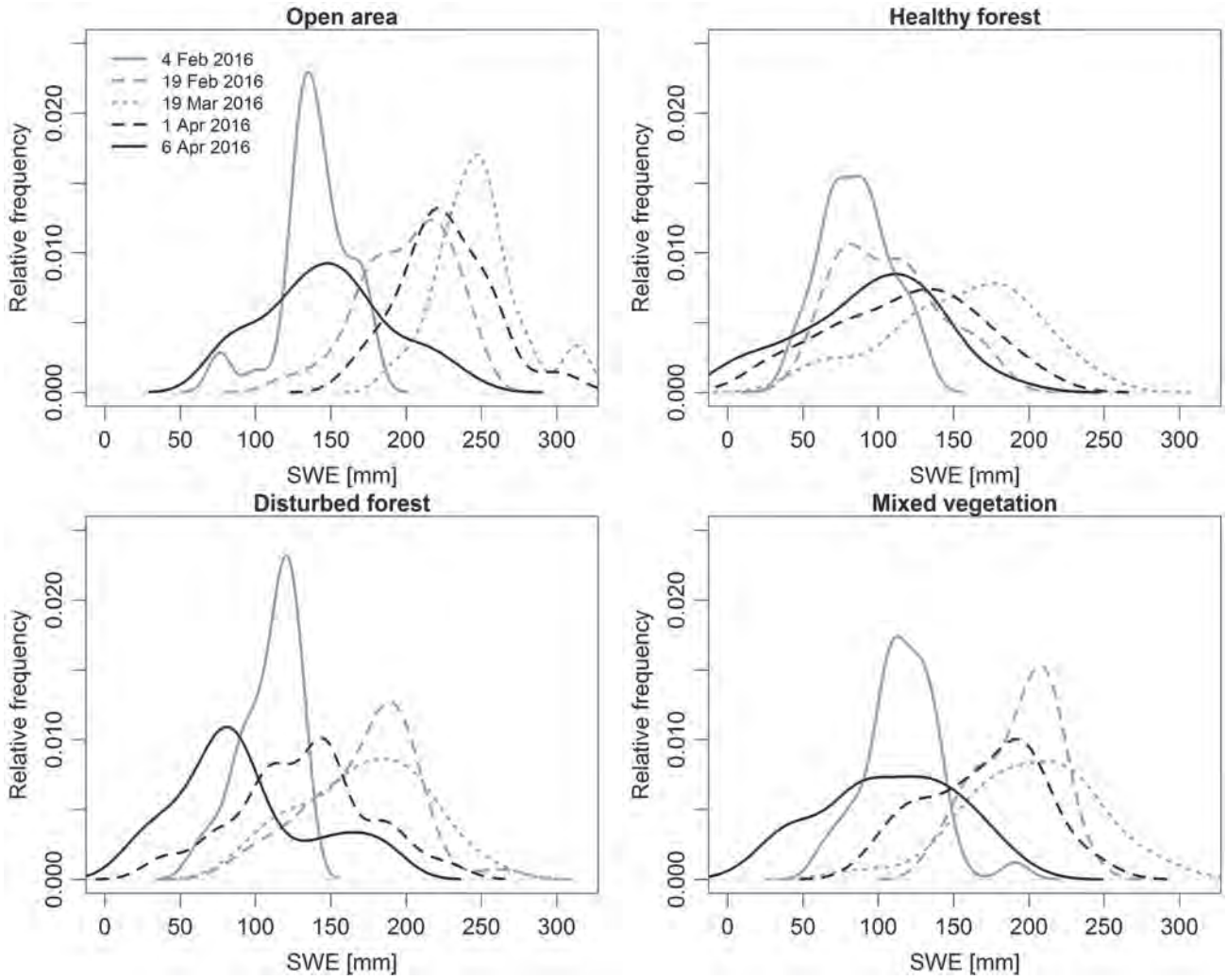

Fig. 5 Histograms of SWE in the time of each data sampling at individual plots. Only points with existing snow cover were included.

Tab. 2 Snowmelt rates, melt factors and relative amount of shortwave radiation compared to open area in individual sampling locations.

Location	Snowmelt rate [mm d^{-1}]	Melt factor m_f [mm $°C^{-1}$ d^{-1}]	M_f relatively compared to open area	Relative amount of shortwave radiation compared to open area
Open area	16.1	3.09	100%	100.0%
Healthy forest	10.9	2.09	68%	6.3%
Disturbed forest	15.0	2.88	93%	23.9%
Mixed vegetation	12.9	2.46	80%	NA

important to mention that the effect of faster snowmelt after forest decline is rather temporary since one can expect increasing shading effects and thus decreasing melt factors during forest regeneration and growth.

As described in the methodology part, the shortwave radiation was measured automatically in plots located in open area, healthy forest and forest disturbed by the bark beetle in order to measure the reduction of shortwave radiation which represents one of the major heat input accessible for snowmelt. The incoming solar radiation in healthy forest decreased to 6.3% of amount typical for open area (due to shading effect) and to 23.9% in disturbed forest compared to open area (Fig. 8).

Calculated melt factors and melt rates confirmed generally know expectations of how the snowmelt is influenced by vegetation and its canopy structure. The canopy structure caused strong decrease in incoming solar radiation and thus melt rates decreased as well. However, the relative decrease in incoming solar radiation in the forest compared to the open area was much bigger compared to the relative decrease in snowmelt rates. This indicated that the decrease in snowmelt rates cannot be explained only by the decrease in incoming solar radiation, and that there are still other processes which accelerated the snowmelt in the forest, such the longwave radiation.

3.4 The modelling of snow accumulation and ablation in plots with different forest type and in the open area

The set-up model was used to simulate the snow accumulation and ablation in all samplings plots (Fig. 9). We performed two separated model runs. First, the model

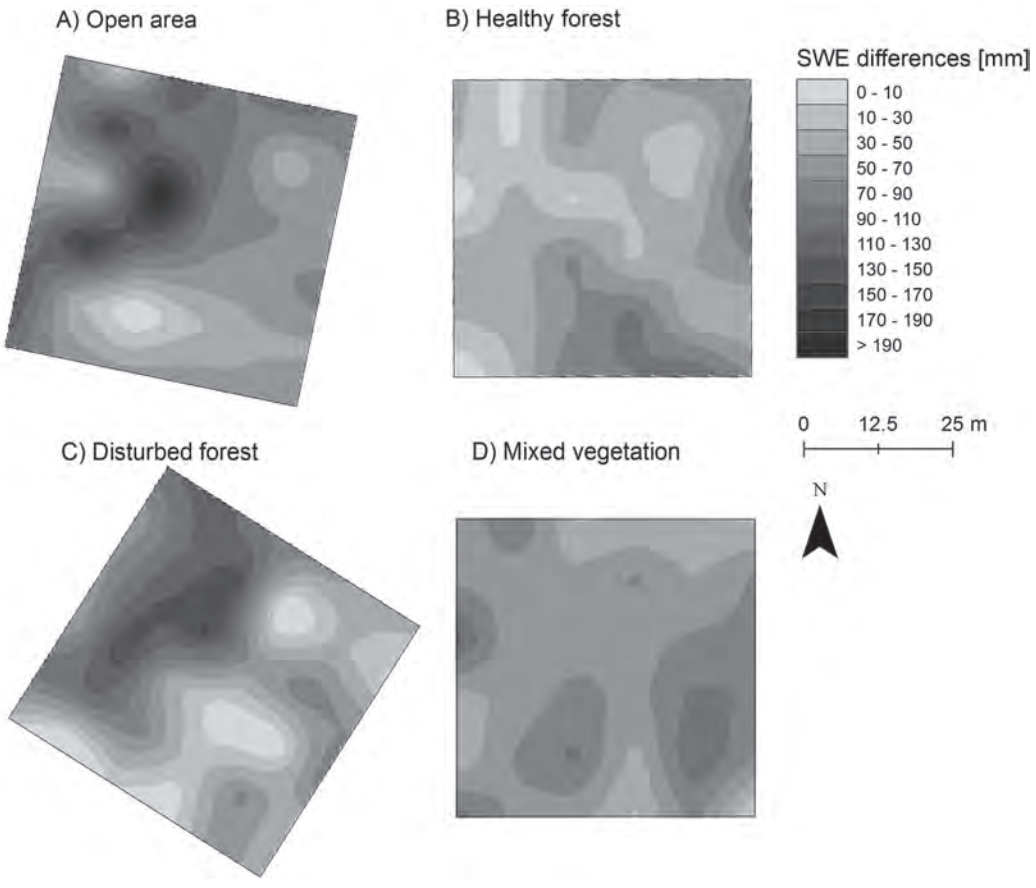

Fig. 6 Snowmelt rates showing the SWE decrease in sampling locations with different vegetation structure between 1 April 2016 and 6 April 2016.

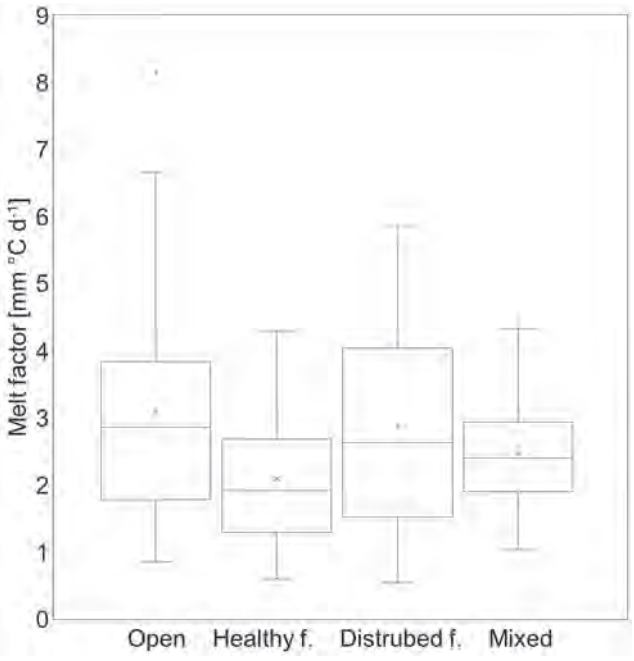

Fig. 7 Melt factors m_f for different vegetation in the sampling locations calculated from measured SWE. Boxes represent 25% and 75% percentile (with median as a thick line), crosses represent mean values and whiskers represent IQR.

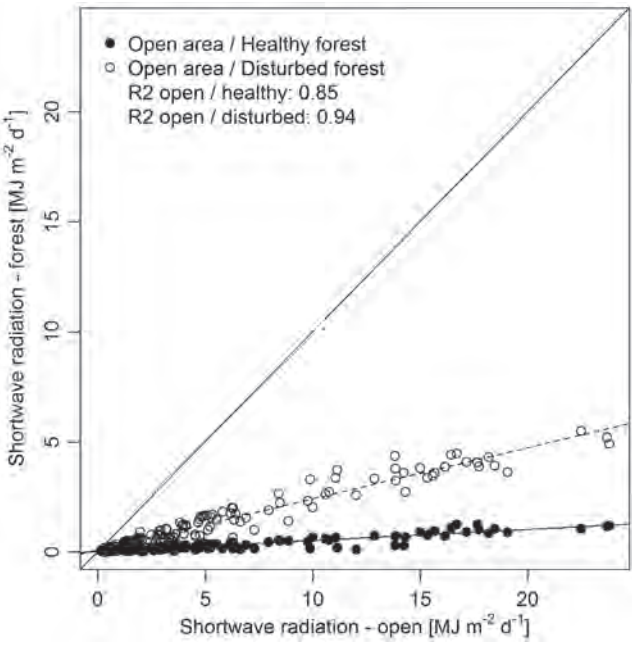

Fig. 8 The daily incoming shortwave radiation measured in open area compared to incoming shortwave radiation measured in healthy forest (black points) and disturbed forest (transparent points) during winter 2015/2016.

started to simulate the SWE at the beginning of the winter season (Fig. 9, left). Second, model simulation started in 19 March 2016 which represents sampling date close to the date with maximum snow storage (Fig. 9, right). The initial values of SWE for the second model run were adjusted in order to represent real measured data. Thus, this model run represents only snowmelt period enabling more detailed look on snowmelt dynamics in different plots with different canopy structure.

The results of the model correspond to general expectation of snow accumulation and snowmelt in different vegetation categories. The results are not surprising since the model was forced to achieved best possible fit with observations (using both manual snow sampling data and the SWE measurement using Snowpack analyzer SPA). The SWE underestimation by the model compared to the SPA data from 12 Jan to 17 Jan (Fig. 9, left) was probably caused by heavy snowfall which was not fully captured by the heated rain gauge in Modrava meteorological station (the record from this rain gauge was used as an input into the model).

The results showed the joint effect of reducing snow accumulation (due to snow interception) and slower snowmelt (due to shortwave radiation) in forest plots and enabled to derive melt-out days (the day of snow disappearance at specific plot). Despite the initial SWE in open area was almost by 60% higher than in the healthy forest when snowmelt began, the melt-out day in the forest was only 4 days earlier than in open area. On the contrary, the melt-out day in disturbed forest was 4 days earlier than in healthy forest despite the higher SWE in the day of snowmelt onset (Fig. 9, right). Faster ablation recorded by the automatic SWE sensor (SPA) was probably caused by the fact that this sensor is placed in open area (however inside the plot D with mixed vegetation) and thus most exposed to solar radiation when comparing all plots.

Tab. 3 Nash-Sutcliffe efficiency used to compare measured and simulated SWE in individual plots.

Location	Nash-Sutcliffe efficiency [–]
Open area	0.92
Healthy forest	0.88
Disturbed forest	0.69
Mixed vegetation	0.73

The model simulated best in open area and slightly worse in healthy forest (Table 3). The worst simulation was achieved in disturbed forest and in plot formed by mixed vegetation. The reason was probably the large SWE variability within the plot caused by large differences in canopy structure. Additionally, in plot with disturbed forest the worst fit may by influenced by inaccurate measured data. This could happen because of many death trees lying in the ground. In such conditions there was very difficult to find representative points for snow depth and SWE measurement. It means, that data measured in disturbed forest are burden with higher portion of uncertainty than data measured in healthy forest and in open area. However, when simulate the SWE in forests sites, the model highlighted the importance to use some factor accounting for snow interception.

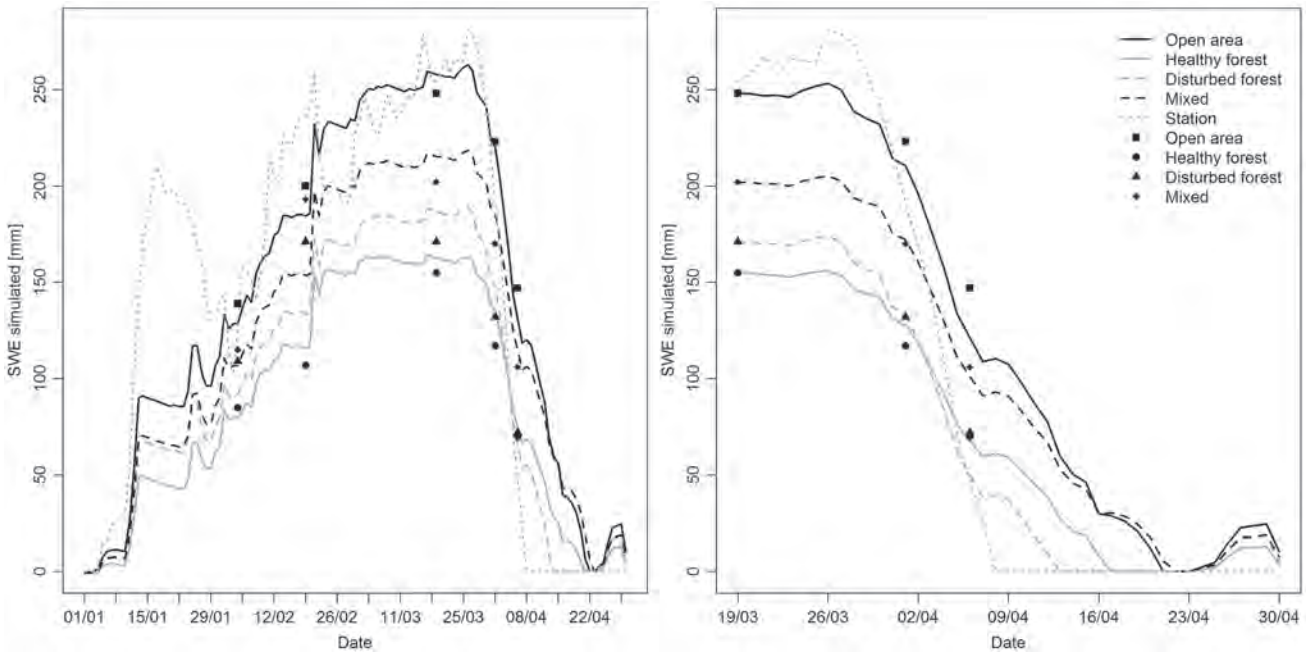

Fig. 9 Simulated SWE from 01 Jan 2016 to 30 Apr 2016 (left). Simulated SWE during snowmelt from 19 Mar 2016 to 30 Apr 2016 (right). Grey line "station" shows the SWE measured by the automatic sensor (SPA).

4. Discussion

4.1 Snow sampling design

The snowpack variability in snow dominated regions is bigger than the variability of precipitation. This is caused by several subsequent processes influencing the snowpack variability after snow accumulation, such as snow redistribution due to wind and earth gravity, snow metamorphosis and snowmelt. All mentioned processes are influenced by meteorological and site conditions which strongly influence individual elements of snowpack energy balance. Site characteristics cause the high snow variability even at a plot scale, where the precipitation may be considered as spatially invariable.

Besides manual sampling design as used in this study a lot of promising results have been also reported using remote sensing approaches such as the use of unmanned aerial systems (UAV) (Lendzioch et al. 2016; Nolan et al. 2015), aerial or terrestrial laser scanning (Bühler et al. 2015; Grünewald et al. 2013; Revuelto et al. 2016) and MODIS satellite data (Duchacek 2014; He et al. 2014; Krajčí et al. 2016). A camera placed on UAV platform was tested to monitor the snow depth characteristics in our study area, more specifically in the plot D with mixed vegetation (Lendzioch et al. 2016).

Selected locations are homogeneous in term of elevation and topography. All localities are placed at the same elevation and they are on a flat area. The only difference between localities is their vegetation cover, influencing interception and the amount of shortwave and longwave radiation. However, both plots located in the healthy forest and disturbed forest are not perfectly homogeneous in term of canopy structure, it means that canopy structure is partly changing within one locality. On the one hand, it represents an advantage because the small scale variability of snow depth and SWE caused by small scale variations of the canopy structure may be assessed. On the other hand, it represents a potential uncertainty when comparing localities between each other; characteristics of the mean were used to describe the snowpack in individual locality. This approach smooths the possible within-plot variations.

Additionally, the snowpack in open area was influenced by surrounding trees, especially on its edges. However, in such forested study area there was not possible to select different plot representing open area which would be large enough to avoid the snowpack distribution influence by surrounding trees. On contrary, the influence of wind on snow redistribution was therefore minimized and thanks to this fact, we argue that spatial snow depth and SWE differences were caused mainly by spatial differences in interception and solar radiation.

4.2 Uncertainties arising from measured meteorological variables

The air temperature used to melt factors calculation and to simulate the snowmelt dynamics was measured at a meteorological station located in the vicinity of sampling plots. Although, air temperature data were automatically measured every 10 minutes, the snow model set-up

in this study used daily temporal resolution which cannot capture small scale variations of air temperature due to the small scale variability of topography. This effect might be important in spring especially in clear sky conditions at night and early morning (frost pockets). Diurnal variations caused that the mean daily air temperature might not be representative to describe snowmelt conditions (if occurred during the day). Local temperature conditions are also affected by the forest structure (Tesař et al. 2006) which is often connected to topography (Hais and Kučera 2009).

The incoming and reflected shortwave radiation was measured in open area, healthy forest and disturbed forest. Since radiometer detectors were not heated, these light detectors were covered with snow in some winter days giving the unreliable data. The identification of such situations was based on simple fact that shortwave radiation from downward facing sensor was higher than from upward facing sensor (which is unlikely in common situations during daylight). If this situation happened, we assumed that the upward facing sensors were covered with snow. Thus, all such measured values were removed from all analysis.

4.3 Vegetation structure and its possible consequences to runoff

For snow dominating regions with significant portion of forested areas, there is a well-documented difference between snow storages in forests and in open areas (see e.g. Holko et al. 2009; Jenicek et al. 2015; Jost et al. 2012; Pomeroy et al. 2012; Šípek and Tesař 2014). The results presented by Jenicek et al. (2016) who performed similar survey of snow storages at a catchment scale (same catchment as in this study) demonstrated similar differences in snow storages accumulated in open areas compared to forest sites (on average by 45% lower snow storages under healthy coniferous forest and 29% by lower snow storage in disturbed forest). On the contrary, Bartík et al. (2014) reported larger decrease of SWE deposited in a disturbed forest compared to open area in the West Tatra Mountains (decrease by 53%).

The melt factors presented in Jenicek et al. (2016) are somewhat higher than in this study, especially for open areas. This might be influenced by previously mentioned fact that open area in this study is rather small and the snowpack distribution might by affected by surrounding trees.

The effect of harvesting was documented by Schelker et al. (2013) who showed the increase in SWE after forest clear-cut by 27% which caused higher runoff from catchment. Additionally, the clear-cutting caused the earlier occurrence of the snowmelt. Pomeroy et al. (2012) performed a wide range of hypothetical scenarios at Marmot Creek in Canada and concluded that the total spring and summer runoff volume increased by less than 10% in case of forest burning and logging, however, the snowmelt volume increases by 45%.

4.4 Simplified snowpack energy balance based on degree-day approach

The snow accumulation and ablation model based on degree-day approach was originally created for daily time resolution and the same temporal resolution was also used in this study. The partial inaccuracies may arise in cases of air temperature fluctuations near zero (Kutlakova and Jenicek 2012). When the mean daily air temperature is negative, the model calculates no snowmelt. However, the positive air temperature which occurred during day might cause partial snowmelt which was not captured by the model (Hock 2003). Although the model allowed for a correction of such situations using critical temperature T_{cmelt}, there is still some portion of uncertainty in simulated snowmelt dynamics.

It is important to mention that only a simplified energy balance was taken into account in the model which means that many processes were not included into calculation, such as latent heat transfers (e.g. water refreezing after liquid precipitation) and longwave radiation. The sublimation and heat flux from earth surface (ground melt) was included in our model, however we used only simplified approach to estimate these two parameters. Further development of the model and testing it on different catchments and/or different years would bring more reliable results.

5. Conclusion

We analyzed the snowpack variability in four selected plots with different land cover in a forested mountain catchment. We were interested in the effect of forest structure on both snow accumulation and ablation. Our study was based on repeated manual measurements of the snow depth and SWE in winter season 2015/2016. Based on results, we draw up following conclusions:

- The snow depth and SWE spatial variability at a plot scale markedly increased during snowmelt season. The variability was generally higher in forest sites than in open area.
- The SWE in the plot with healthy forest was on average by 41% lower than in open area during snow accumulation period. The disturbed forest caused the SWE reduction by 22% compared to open area indicating reducing snow interception after forest defoliation and thus increasing snow storage.
- The snow ablation in healthy forest was by 32% slower compared to open area. On the contrary, the snow ablation in disturbed forest (due to the bark beetle) was on average only by 7% slower than in open area. The dominant process which explains mentioned differences is reduced amount of incoming shortwave radiation in forested sites.
- The measured incoming solar radiation in healthy forest decreased to 6.3% of amount measured in open

area in the same period and to 23.9% in disturbed forest compared to open area. However, the relative decrease in incoming solar radiation in the forest compared to open area was much bigger compared to the relative decrease in snowmelt rates. This indicated that the decrease in snowmelt rates cannot be explained only by the decrease in incoming solar radiation.

– The results of the model showed the joint effect of reducing snow accumulation (due to snow interception) and slower snowmelt (due to shortwave radiation) in forest plots and enabled to derive melt-out days at individual plots. Despite the initial SWE in disturbed forest was by 10% higher than in the healthy forest when snowmelt began, the melt-out day in the disturbed forest was by 4 days earlier then in the healthy forest. The model simulated best in open area and slightly worse in healthy forest. The worst simulation was achieved in disturbed forest and in the plot formed by mixed vegetation.

Acknowledgements

Support from the Czech Science Foundation (project No. 13-32133S "Headwaters retention potential with respect to hydrological extremes") and European Union (project EU COST Action 1306, no. LD15130 "Impact of landscape disturbance on the stream and basin connectivity") is gratefully acknowledged.

REFERENCES

AUBIN, I., BEAUDET, M., MESSIER, C. (2011): Light extinction coefficients specific to the understory vegetation of the southern boreal forest, Quebec. Can. J. For. Res. 30, 168–177. https://doi.org/10.1139/x99-185

BARTÍK, M., SITKO, R., OREŇÁK, M., SLOVIK, J., ŠKVARENINA, J. (2014): Snow accumulation and ablation in disturbed mountain spruce forest in West Tatra Mts. Biologia (Bratisl). 69, 1492–1501. https://doi.org/10.2478/s11756-014-0461-x

BIEDERMAN, J. A., BROOKS, P. D., HARPOLD, A. A., GOCHIS, D. J., GUTMANN, E., REED, D. E., PENDALL, E., EWERS, B. E. (2014): Multiscale observations of snow accumulation and peak snowpack following widespread, insect-induced lodgepole pine mortality. Ecohydrology 7, 150–162. https://doi.org/10.1002/eco.1342

BÜHLER, Y., MARTY, M., EGLI, L., VEITINGER, J., JONAS, T., THEE, P., GINZLER, C. (2015): Snow depth mapping in high-alpine catchments using digital photogrammetry. Cryosph. 9, 229–243. https://doi.org/10.5194/tc-9-229-2015

DUCHACEK, L. (2014): Vertical variability in the position of the zero isochion in geomorphologic regions of Czechia. Geografie 119, 145–160.

ELLIS, C. R., POMEROY, J. W. (2007): Estimating sub-canopy shortwave irradiance to melting snow on forested slopes. Hydrol. Process. 21, 2581–2593. https://doi.org/10.1002/hyp.6794

ESSERY, R., POMEROY, J., PARVIAINEN, J., STORCK, P. (2003): Sublimation of Snow from Coniferous Forests in a Climate Model. J. Clim. 16, 1855–1864. https://doi.org/10.1175/1520-0442(2003)016<1855:SOSFCF>2.0.CO;2

GRÜNEWALD, T., STÖTTER, J., POMEROY, J. W., DADIC, R., MORENO BAÑOS, I., MARTURIÀ, J., SPROSS, M., HOPKINSON, C., BURLANDO, P., LEHNING, M. (2013): Statistical modelling of the snow depth distribution in open alpine terrain. Hydrol. Earth Syst. Sci. 17, 3005–3021. https://doi.org/10.5194/hess-17-3005-2013

HAIS, M., KUČERA, T. (2009): The influence of topography on the forest surface temperature retrieved from Landsat TM, ETM + and ASTER thermal channels. ISPRS J. Photogramm. Remote Sens. 64, 585–591. https://doi.org/10.1016/j.isprsjprs.2009.04.003

HE, Z. H., PARAJKA, J., TIAN, F. Q., BLÖSCHL, G. (2014): Estimating degree-day factors from MODIS for snowmelt runoff modeling. Hydrol. Earth Syst. Sci. 18, 4773–4789. https://doi.org/10.5194/hess-18-4773-2014

HOCK, R. (2003): Temperature index melt modelling in mountain areas. J. Hydrol. 282, 104–115. https://doi.org/10.1016/S0022-1694(03)00257-9

HOLKO, L., ŠKVARENINA, J., KOSTKA, Z., FRIČ, M., STAROŇ, J. (2009): Impact of spruce forest on rainfall interception and seasonal snow cover evolution in the Western Tatra Mountains, Slovakia. Biologia (Bratisl). 64, 594–599. https://doi.org/10.2478/s11756-009-0087-6

HRIBIK, M., VIDA, T., SKVARENINA, J., SKVARENINOVA, J., IVAN, L. (2012): Hydrological effects of norway spruce and european beech on snow cover in a mid-mountain region of the Polana Mts., Slovakia. J. Hydrol. Hydromechanics 60, 319–332.

JENICEK, M., BEITLEROVA, H., HASA, M., KUCEROVA, D., PEVNA, H., PODZIMEK, S. (2012): Modeling snow accumulation and snowmelt runoff – present approaches and results. AUC Geographica 47, 15–24.

JENICEK, M., PEVNA, H., MATEJKA, O. (2016): Canopy structure and topography effects on snow distribution at a catchment scale: Application of multivariate approaches. J. Hydrol. Hydromechanics. Submitted.

JENICEK, M., PEVNA, H., MATEJKA, O. (2015): Snow accumulation and ablation in three forested mountain catchments. Acta Hydrol. Slovaca 16, 208–216.

JOST, G., DAN MOORE, R., SMITH, R., GLUNS, D.R. (2012): Distributed temperature-index snowmelt modelling for forested catchments. J. Hydrol. 420, 87–101. https://doi.org/10.1016/j.jhydrol.2011.11.045

JOST, G., WEILER, M., GLUNS, D.R., ALILA, Y. (2007): The influence of forest and topography on snow accumulation and melt at the watershed-scale. J. Hydrol. 347, 101–115. https://doi.org/10.1016/j.jhydrol.2007.09.006

KLIMENT, Z., MATOUSKOVA, M., LEDVINKA, O., KRALOVEC, V. (2011): Trend Analysis of Rainfall-Runoff Regimes in Selected Headwater Areas of the Czech Republic. J. Hydrol. Hydromechanics 59, 36–50. https://doi.org/10.2478/v10098-011-0003-y

KOCUM, J., OULEHLE, F., JANSKÝ, B., BŮZEK, F., HRUŠKA, J., VLČEK, L. (2016): Geochemical evidence for peat bog contribution to the streamflow generation process: case study of the Vltava River headwaters, Czech Republic. Hydrol. Sci. J. 61, 1–11. https://doi.org/10.1080/02626667.2016.1140173

KRAJČÍ, P., HOLKO, L., PARAJKA, J. (2016): Variability of snow line elevation, snow cover area and depletion in the main Slovak basins in winters 2001–2014. J. Hydrol. Hydromechanics 64, 12–22. Hydromechanics 64, 12–22. https://doi.org/10.1515/johh-2016-0011

KUTLAKOVA, L., JENICEK, M. (2012): Modelling snow accumulation and snowmelt in the Bystrice River basin. Geografie 117, 110–125.

LANGHAMMER, J., HARTVICH, F., KLIMENT, Z., JENÍČEK, M., BERNSTEINOVÁ, J., VLČEK, L., SU, Y., ŠTYCH, P., MIŘIJOVSKÝ, J. (2015a):. The impact of disturbance on the dynamics of fluvial processes in mountain landscapes. Silva Gabreta 21, 105–116.

LANGHAMMER, J., SU, Y., BERNSTEINOVÁ, J. (2015b): Runoff Response to Climate Warming and Forest Disturbance in a Mid-Mountain Basin. Water 7, 3320–3342. https://doi.org/10.3390/w7073320

LENDZIOCH, T., LANGHAMMER, J., JENICEK, M. (2016): Tracking forest and open area effects on snow accumulation by unmanned aerial vehicle photogrammetry. ISPRS - International Archives of the Photogrammetry, Remote Sensing and Spatial Information Sciences XLI-B1, 917–923. https://doi.org/10.5194/isprsarchives-XLI-B1-917-2016

LÓPEZ-MORENO, J. I., STÄHLI, M. (2008): Statistical analysis of the snow cover variability in a subalpine watershed: Assessing the role of topography and forest interactions. J. Hydrol. 348, 379–394. https://doi.org/10.1016/j.jhydrol.2007.10.018

MOLOTCH, N. P., BROOKS, P. D., BURNS, S. P., LITVAK, M., MONSON, R. K., MCCONNELL, J. R., MUSSELMAN, K. (2009): Ecohydrological controls on snowmelt partitioning in mixed-conifer sub-alpine forests. Ecohydrology 2, 129–142. https://doi.org/10.1002/eco.48

NASH, J. E., SUTCLIFFE, J. V. (1970): River flow forecasting through conceptual models part I – A discussion of principles. J. Hydrol. 10, 282–290. https://doi.org/10.1016/0022-1694(70)90255-6

NOLAN, M., LARSEN, C., STURM, M. (2015): Mapping snow depth from manned aircraft on landscape scales at centimeter resolution using structure-from-motion photogrammetry. Cryosph. 9, 1445–1463. https://doi.org/10.5194/tc-9-1445-2015

POMEROY, J., FANG, X., ELLIS, C. (2012): Sensitivity of snowmelt hydrology in Marmot Creek, Alberta, to forest cover disturbance. Hydrol. Process. 26, 1891–1904. https://doi.org/10.1002/hyp.9248

R CORE TEAM (2016): A language and environment for statistical computing. R Foundation for Statistical Computing, Vienna, Austria. URL https://www.r-project.org/ (accessed 8.1.16).

REVUELTO, J., VIONNET, V., LÓPEZ-MORENO, J. I., LAFAYSSE, M., MORIN, S. (2016): Combining snowpack modeling and terrestrial laser scanner observations improves the simulation of small scale snow dynamics. J. Hydrol. 533, 291–307. https://doi.org/10.1016/j.jhydrol.2015.12.015

SCHELKER, J., KUGLEROVÁ, L., EKLÖF, K., BISHOP, K., LAUDON, H. (2013): Hydrological effects of clear-cutting in a boreal forest – Snowpack dynamics, snowmelt and streamflow responses. J. Hydrol. 484, 105–114. https://doi.org/10.1016/j.jhydrol.2013.01.015

SICART, J. E., ESSERY, R. L. H., POMEROY, J. W., HARDY, J., LINK, T., MARKS, D. (2004): A Sensitivity Study of Daytime Net Radiation during Snowmelt to Forest Canopy and Atmospheric Conditions. J. Hydrometeorol. 5, 774–784. https://doi.org/10.1175/1525-7541(2004)005<0774:ASSODN>2.0.CO;2

STÄHLI, M., GUSTAFSSON, D. (2006): Long-term investigations of the snow cover in a subalpine semi-forested catchment. Hydrol. Process. 20, 411–428. https://doi.org/10.1002/hyp.6058

ŠÍPEK, V., TESAŘ, M. (2014): Seasonal snow accumulation in the mid-latitude forested catchment. Biologia (Bratisl). 69, 1562–1569. https://doi.org/10.2478/s11756-014-0468-3

TESAŘ, M., ŠÍR, M., LICHNER, L., ZELENKOVÁ, E. (2006): Influence of vegetation cover on thermal regime of mountainous catchments. Biologia (Bratisl). 61, 311–314. https://doi.org/10.2478/s11756-006-0179-5

VARHOLA, A., COOPS, N. C., WEILER, M., MOORE, R. D. (2010): Forest canopy effects on snow accumulation and ablation: An integrative review of empirical results. J. Hydrol. 392, 219–233. https://doi.org/10.1016/j.jhydrol.2010.08.009

RESUMÉ

Akumulace a úbytek sněhu v různých vegetacích v lokálním měřítku: použití přístupu degree-day a měřené krátkovlnné radiace

Informace o objemu vody ve sněhové pokrývce a jejím prostorovém rozložení jsou důležité pro předpovědi odtoku z tajícího sněhu. Cílem této studie bylo kvantifikovat vliv různé struktury lesního porostu na prostorové rozložení sněhové pokrývky v lokálním měřítku během akumulace a tání sněhu. Dílčí zájem představoval vliv lesa poškozeného lýkožroutem smrkovým (*Ips typographus*).

Na vybraných malých horských plochách byla v zimní sezóně 2015/2016 provedena opakovaná detailní měření výšky sněhu a vodní hodnoty sněhu (SWE). Jednotlivé plochy se nacházely blízko sebe ve stejné nadmořské výšce bez vlivu reliéfu a větru na rozložení sněhu. Tím bylo možné sledovat pouze efekt vegetace (ovlivňující intercepci sněhu a radiační podmínky) na distribuci sněhu. Byl sestaven model akumulace a úbytku sněhu, který simuloval průběh SWE na vybraných plochách. Model by založen na přístupu degree-day a zohledňoval intercepci sněhu v různých strukturách vegetace. Model byl kalibrován jak na manuálně měřených hodnotách SWE, tak na datech z automatické stanice umístěné v blízkosti ploch a měřící kromě srážek a teploty vzduchu také výšku sněhu, SWE a globální a odraženou krátkovlnnou radiaci.

Měření ukázala, že SWE ve zdravém lese byla době akumulace sněhu v průměru o 41 % nižší, než na otevřené ploše. Naproti tomu, poškozený les způsobil pouze o 22 % nižší akumulaci sněhu než na otevřené ploše. Ve zdravém lese bylo naměřeno o 32 % pomalejší tání sněhu ve srovnání s otevřenou plochou. Naproti tomu, v poškozeném lese bylo tání pouze o 7 % pomalejší než na otevřené ploše, což lze vysvětlit vyšším úhrnem krátkovlnného záření dopadající na plochu po rozpadu lesa. Avšak pokles krátkovlnné radiace jak ve zdravém, tak poškozeném lese je mnohem vyšší než by vysvětloval pokles rychlosti tání sněhu. To ukazuje na fakt, že krátkovlnná radiace nemůže sama vysvětlit změnu v tání sněhu po rozpadu lesa. Sestavený a kalibrovaný model očekávaně modeloval nejpřesněji průběh SWE na otevřené ploše, o něco hůře ve zdravém a poškozeném lese. Model prokázal obecně zrychlení tání sněhu po rozpadu lesa, což mělo také za následek rychlejší roztátí sněhu na ploše s poškozeným lesem (navzdory vyšším sněhovým zásobám na počátku tání sněhu).

Michal Jeníček, Ondřej Hotový, Ondřej Matějka
Charles University, Faculty of Science
Department of Physical Geography and Geoecology,
Albertov 6, 128 43 Prague
Czech Republic
E-mail: michal.jenicek@natur.cuni.cz